JACS Au
AN OPEN ACCESS JOURNAL OF THE AMERICAN CHEMICAL SOCIETY

pubs.acs.org/jacsau
Article

Enabling Universal Access to Rapid and Stable Tetrazine Bioorthogonal Probes through Triazolyl-Tetrazine Formation

Haojie Yang, Hongbao Sun, Yinghan Chen, Yayue Wang, Cheng Yang, Fang Yuan, Xiaoai Wu, Wei Chen, Ping Yin, Yong Liang,* and Haoxing Wu*

Cite This: JACS Au 2024, 4, 2853−2861
Read Online

ACCESS | Metrics & More | Article Recommendations | Supporting Information

ABSTRACT: Despite the immense potential of tetrazine bioorthogonal chemistry in biomedical research, the in vivo performance of tetrazine probes is challenged by the inverse correlation between the physiological stability and reactivity of tetrazines. Additionally, the synthesis of functionalized tetrazines is often complex and requires specialized reagents. To overcome these issues, we present a novel tetrazine scaffold—triazolyl-tetrazine—that can be readily synthesized from shelf-stable ethynyl-tetrazines and azides. Triazolyl-tetrazines exhibit improved physiological stability along with high reactivity. We showcase the effectiveness of this approach by creating cell-permeable probes for protein labeling and live cell imaging, as well as efficiently producing ^{18}F-labeled molecular probes for positron emission tomography imaging. By utilizing the readily available pool of functionalized azides, we envisage that this modular approach will provide universal accessibility to tetrazine bioorthogonal tools, facilitating applications in biomedicine and materials science.

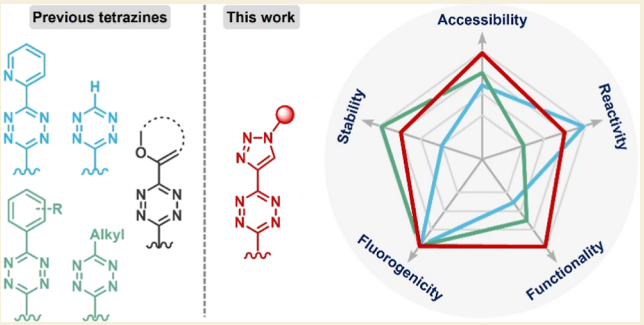

KEYWORDS: *tetrazine, bioorthogonal chemistry, modular synthesis, click chemistry, imaging*

INTRODUCTION

Bioorthogonal chemistry,[1−4] a strategy first proposed in 2000,[5] has revolutionized various fields, including chemical biology, drug discovery, molecular imaging, and biomaterials. As the applications of bioorthogonal chemistry continue to expand, optimizing the bioorthogonality of reaction tools has become increasingly important. Remaining challenges include optimizing the reactant structure to enhance their stability and prevent degradation in a biological milieu;[1] improving the reaction kinetics to facilitate biomedical applications at low concentrations;[6,7] developing bioorthogonal "mini-tags" to avoid interfering with normal cellular processes;[8] creating bioorthogonal cleavage reactions for selective activation or drug release;[9−14] and designing bioorthogonal fluorogenic probes for in vivo imaging.[15]

Achieving the optimal balance between stability and rapid reaction kinetics of reactants is crucial for their in vivo performance,[1] but it remains highly challenging. The reactants must remain inert to all species in the living system while remaining highly reactive toward their bioorthogonal reaction partners (Figure 1A). Particularly for certain in vivo biomedical applications, the kinetic constants should be greater than 10^4 M^{-1} s^{-1} to enable conjugation at diagnostic or therapeutic concentrations,[1,16,17] while the reactants must remain stable after tens of hours in the circulation. The inverse electron-demand Diels−Alder (IEDDA) reaction between tetrazine and *trans*-cyclooctene (TCO) has been recognized as the most rapid bioorthogonal reaction,[18,19] demonstrating successful applications in animal models and clinical transformative potential.[14,20,21] Various probes or theranostic agents based on this chemistry have been developed for diverse cutting-edge applications, including super-resolution imaging of biomolecules in live cells, site-specific protein multimodification or function regulation, on-demand prodrug release, and pretargeted nuclear imaging and radionuclide therapy.[13,17,22−26] However, the inverse correlation between the stability and reactivity of these reactants greatly limits their bioorthogonal performance in living systems and clinic translation.[1,16]

It has long been recognized that electron deficiency accelerates the IEDDA reaction but can also lead to loss of stability[1,16,27] (Figure 1B). For instance, while monosubstituted tetrazine and pyridyl-tetrazine react extremely rapidly with dienophiles, they degrade relatively quickly in the cellular environment. In contrast, alkyl- and phenyl-substituted tetrazines are usually more stable and easier to functionalize,

Received: December 29, 2023
Revised: May 7, 2024
Accepted: May 16, 2024
Published: May 30, 2024

https://doi.org/10.1021/jacsau.3c00843
JACS Au 2024, 4, 2853−2861

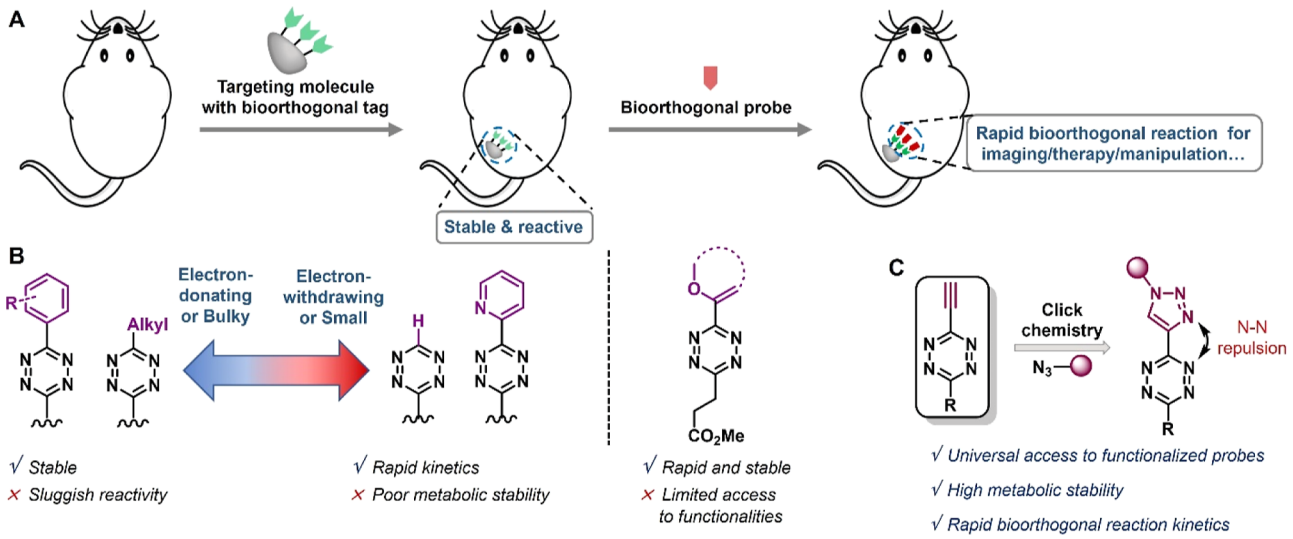

Figure 1. (A) General principle of utilizing bioorthogonal reporters for in vivo bioconjugation. (B) Previous tetrazine skeletons and their advantages and limitations. (C) Our design strategy for universal access to rapid and stable bioorthogonal probes.

but their relative sluggish in vivo reactivity makes them poorly suited for detecting low-abundance targets. The only exception is the vinylether tetrazines, which were reported recently by the Fox group and which exhibited rapid kinetics bearing an electron-donating substituent (Figure 1B).[28] Subsequent mechanistic studies by Mikula et al. revealed that intramolecular repulsion also plays a key role in the IEDDA reaction kinetics in this system.[29] These findings suggest that rational design could be utilized to optimize the stability and reactivity of tetrazines.

Another long-standing issue in tetrazine bioorthogonal chemistry is the accessibility of functionalized tetrazine probes. While several *de novo* synthetic methodologies[30−32] or postmodification cross-coupling strategies[28,33−36] have recently been developed to generate unsymmetrical functionalized tetrazines, all of these synthetic approaches require extensive synthetic skills or restricted materials, which hampers their use in many biochemical and biomedical research centers.

To address these challenges, this study aims to develop a new molecular design strategy for stable and reactive tetrazines with comprehensive functional group accessibility. Our approach involves the use of a triazolyl-tetrazine scaffold, which we believe will provide an ideal novel skeleton (Figure 1C). The intramolecular electron-pair repulsion between nitrogen atoms on the triazolyl and tetrazine is expected to promote bioorthogonal kinetics. Additionally, the 1,4-triazole substituent is a weak inductively electron-withdrawing group[37] that can enhance the physiological stability of the tetrazine, as compared to pyridyl- or monosubstituted tetrazines. Therefore, we also hypothesize that the modular synthesis of triazolyl-tetrazine can be achieved through a copper-catalyzed azide−alkyne click reaction (CuAAC) using ethynyl-tetrazine precursors. We anticipate that this strategy will be straightforward to implement and given the wide variety of commercially available functionalized azides, will lead to the creation of a versatile range of tetrazine bioorthogonal probes.

RESULTS AND DISCUSSION

To test our hypotheses, our first goal was to develop a simple methodology for preparing ethynyl-tetrazine since only a few reports exist describing alkynyl-tetrazines[38,39] and ethynyl-tetrazines are unknown. To achieve this, we focused on a recently developed 3-methylthiotetrazine[28] that can be prepared from corresponding carboxylic esters in two steps with wide functionality tolerance. This approach allows us to avoid the use of restrictive reagents such as anhydrous hydrazine. We envisaged that this versatile precursor could be used for preparing ethynyl-tetrazine through a Liebeskind−Srogl reaction. Our initial attempt involved reacting 3-(methylthio)-6-phenyl-1,2,4,5-tetrazine (**1**) as the model substrate and tributyl(trimethylsilylethynyl)stannane as the nucleophile, using palladium-catalysis conditions with copper iodide. We obtained the desired TMS-protected ethynyl-tetrazine product in a moderate yield of 52% (Supporting Information, Table S1). After exploring different catalysts, copper additives, and temperatures, we discovered the best reaction conditions involved 0.2 equiv of $PdCl_2(PPh_3)_2$ as catalyst and 2.0 equiv of CuI, resulting in a 91% product yield and 83% on a gram scale (Supporting Information, Table S1). After flash column purification and deprotection of the TMS group under slightly alkaline conditions, ethynyl-tetrazine **2a** was produced in 70% overall yield (Scheme 1). We obtained **2a** as a red crystalline solid, and it remained stable for at least 150 days at 4 °C (Supporting Information, Figure S1).

This synthetic approach was determined to have a wide substrate scope (Scheme 1). We successfully generated an array of ethynyl-tetrazines (**2b−2i**) bearing different functionalized phenyl groups or heterocycles at the 3-position in two-step isolated yields of 48−73%. We also obtained alkyl-substituted ethynyl-tetrazines bearing ether, ester, amide, or amino acid "handles" in yields of 29−51% (**2j−2m**).

Encouraged by the aforementioned results, efforts shifted toward utilizing click chemistry with these ethynyl-tetrazines to generate tetrazines for use as biomedical probes (Scheme 2). We obtained desired triazole product **3a** in an isolated yield of 97% by reacting **2a** with a simple azide, ethyl azidoacetate, under well-established CuAAC conditions.[40,41] We adjusted the hydrophilicity of the tetrazines through PEGylation with functional handles (**3b−3g**) and obtained the tetrazine dimer **3i** with a disulfide linkage in good yield so that it could be applied for the development of cleavable materials. We also added different functional handles to tetrazine to generate

https://doi.org/10.1021/jacsau.3c00843
JACS Au 2024, 4, 2853−2861

Scheme 1. Preparation of Ethynyl-Tetrazines and Substrate Scope[a]

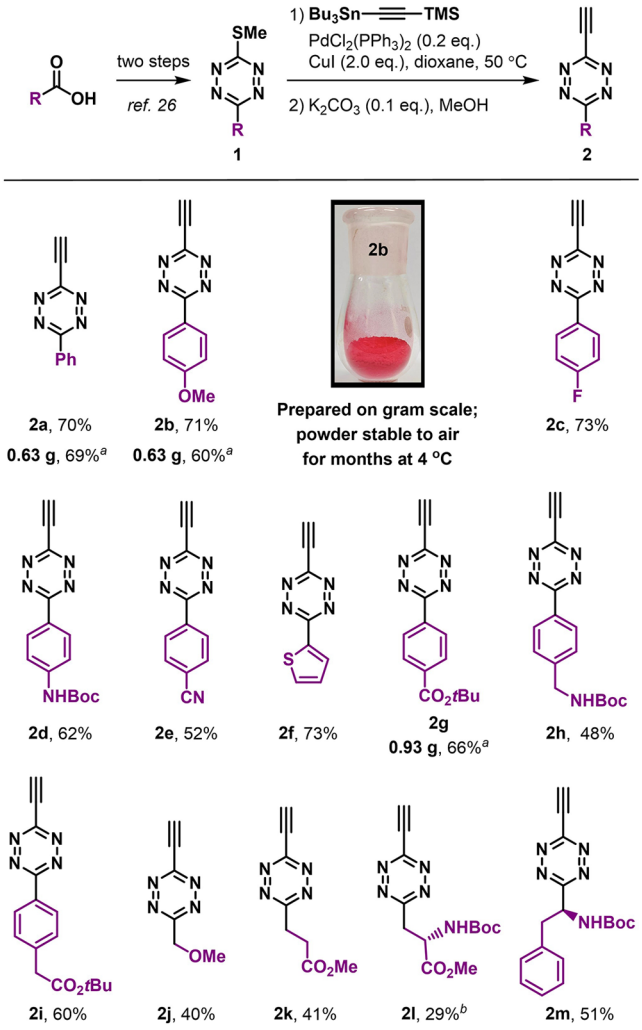

[a]Yields of isolated products are based on **1**. Reactions were conducted under standard conditions on a 0.2 mmol scale, unless otherwise noted. [b]5 mmol scale. [c]80 °C, 2 h for the coupling step.

molecular probes, such as a photoreactive diazirine (**3h**), an ammonium salt (**3j**), a fluorophore with an ester (**3l**), biotin (**3m**), and α-lipoic acid (**3n**).

To ensure the safety of the synthesized triazolyl-tetrazines during laboratory operations, we conducted a differential scanning calorimetry experiment to investigate the thermal behavior of compounds **3a** and **3h**, both of which are relatively nitrogen-rich among the compounds we have developed. To our satisfaction, we observed slow thermal decomposition, supported by a gradual exothermic decomposition process lasting over 5 min (Supporting Information, Figure S24). This suggests the excellent safety of triazolyl-tetrazines.[42,43]

Having developed various functionalized triazolyl-tetrazines, we aimed to assess the bioorthogonal performance of the triazolyl-tetrazines in terms of their stability and reaction kinetics. For our reference compound, we used compound **3b**, which features a commonly used benzoic acid functional group. We then compared it against tetrazines in which the triazolyl group was replaced with hydrogen, methyl, phenyl, or pyridyl while maintaining the same benzoic acid substituents at the 6-position (Figure 2A). We incubated the five compounds at 37 °C in Dulbecco's modified Eagle medium (DMEM) containing 10% fetal bovine serum (FBS) to determine their stability. We observed rapid loss of absorption of the tetrazine chromophore by liquid chromatography (LC)−mass spectrometry in the case of pyridyl- (**Py-Tz**) or H-tetrazine (**H-Tz**), with less than 13% of the compounds remaining after 48 h (Figure 2B). Conversely, **3b** and methyl-tetrazine (**Me-Tz**) showed much greater stability, with more than 92% of the starting compounds still present after 12 h and at least 63% present after 48 h. Similar results were obtained when we incubated the compounds in pure FBS (Supporting Information, Table S3 and Figure S12). Our findings indicated that the triazolyl-tetrazines exhibit good stability under physiological conditions against metabolic decomposition, even after prolonged incubation.

To effectively function as bioorthogonal probes, tetrazines must possess sufficient stability to persist in the body for a certain period, while also displaying sufficient reactivity to rapidly and completely undergo the desired chemistry in vivo. We determined the second-order rate constant for the reactions between different tetrazines and axial-TCO (4a-TCO). The rate constant for **3b** was determined as 10332 M^{-1} s^{-1}, which is slower than that for pyridyl-tetrazine (**Py-Tz**) but still within the same order of magnitude. Moreover, it was at least 6-fold higher than those for phenyl- (**Ph-Tz**) or methyl-tetrazine (**Me-Tz**) (Figure 2C). Notably, **3b** reacted quite fast for such a stable tetrazine derivative (Figure 2D), confirming our hypothesis that rational design could avoid the compromise between stability and reactivity that has long hampered the biomedical application of tetrazine bioorthogonal chemistry. Furthermore, in the presence of a more reactive but slightly less stable conformationally strained dienophile (*cis*-dioxolane-fused TCO, *d*-TCO),[21] the rate constant of **3b** at ambient temperature was determined as 39406 M^{-1} s^{-1} using stopped-flow spectrophotometry (Figure 2E).

To understand the high reactivity and good stability of triazolyl-tetrazines (**Ta-Tz**), we conducted density functional theory calculations to analyze the superiority of the triazolyl substituent as compared to phenyl and pyridyl substituents (Figure 3). According to the frontier molecular orbital theory, in the IEDDA reaction, a lower lowest unoccupied molecular orbital (LUMO) energy of the tetrazine corresponds to a higher reaction rate.[16,29,45] **Py-Tz** exhibits the lowest LUMO level (0.46 eV), consistent with its lowest activation free-energy barrier for the cycloaddition of **Py-Tz** and TCO. However, the comparison between **Ta-Tz** and **Ph-Tz** showed that **Ta-Tz**, possessing a higher vacant orbital energy (0.64 versus 0.56 eV), exhibited greater reactivity than **Ph-Tz** (14.6 versus 15.0 kcal mol^{-1}) due to intramolecular repulsion (Figure 3A,B).[29] To reveal the origin of the observed reactivity, we performed distortion/interaction analysis[46−48] on three transition states involving **Ph-Tz**, **Ta-Tz**, and **Py-Tz**. In this analysis, the activation energy ($\Delta E^{\ddagger}$) comprises two parts: the distortion energy (ΔE_{dist}) associated with the structural distortion that the reactants must undergo to reach their transition-state geometry and the interaction energy (ΔE_{int}) arising from the approach of increasingly distorted reactants. Although the interaction energies of these three reactions were calculated to be approximately equal, the activation energies for **Ta-Tz** and **Py-Tz** were much lower than that in the case of **Ph-Tz**, which can be attributed to their reduced distortion energies (Figure 3C). For the most reactive **Py-Tz**, the total

https://doi.org/10.1021/jacsau.3c00843
JACS Au 2024, 4, 2853−2861

Scheme 2. Modular Access of Triazolyl-Tetrazine Probes with Biomedical Functionalities[a]

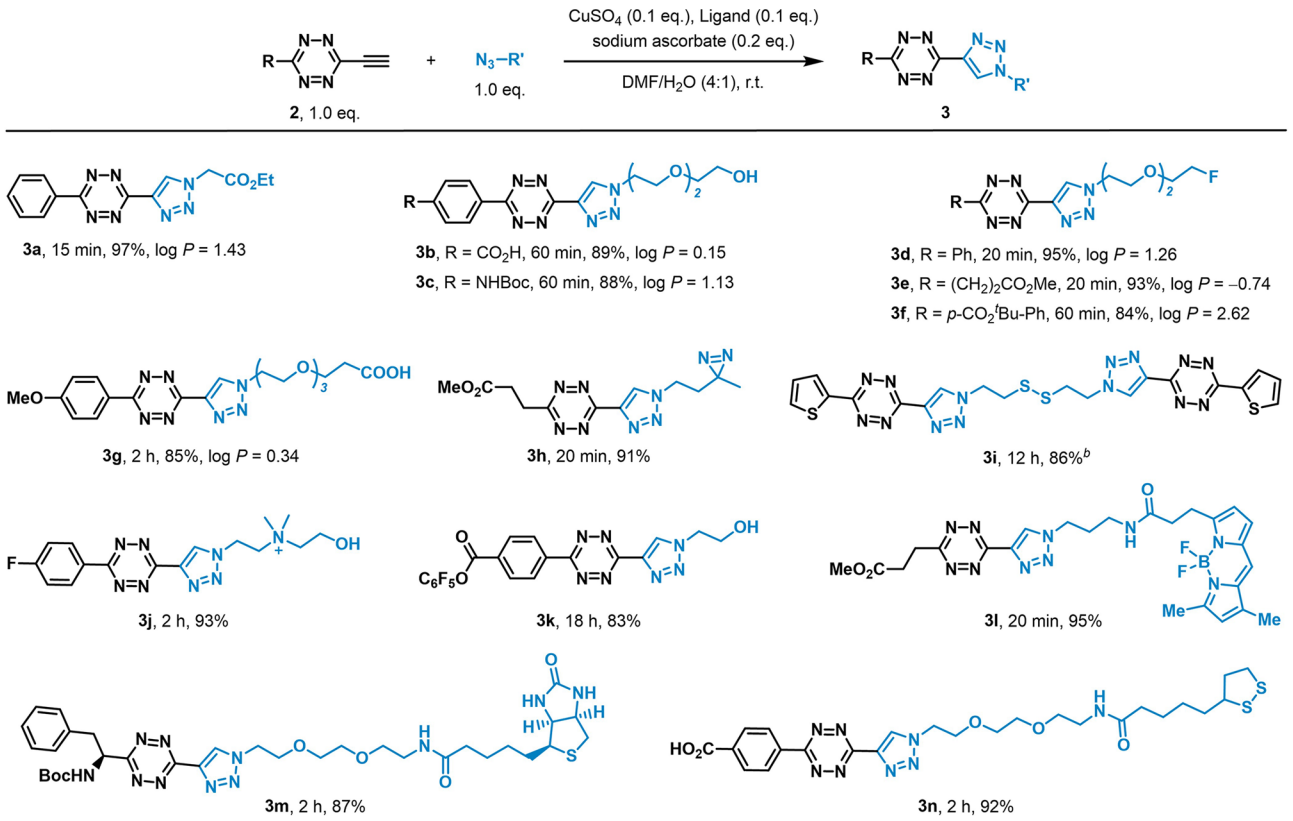

[a]Reaction times and isolated yields are shown under each product. The predicted octanol/water partition coefficient (log *P*) was calculated using the software Molinspiration property calculator. [b]0.5 equiv of azide was used.

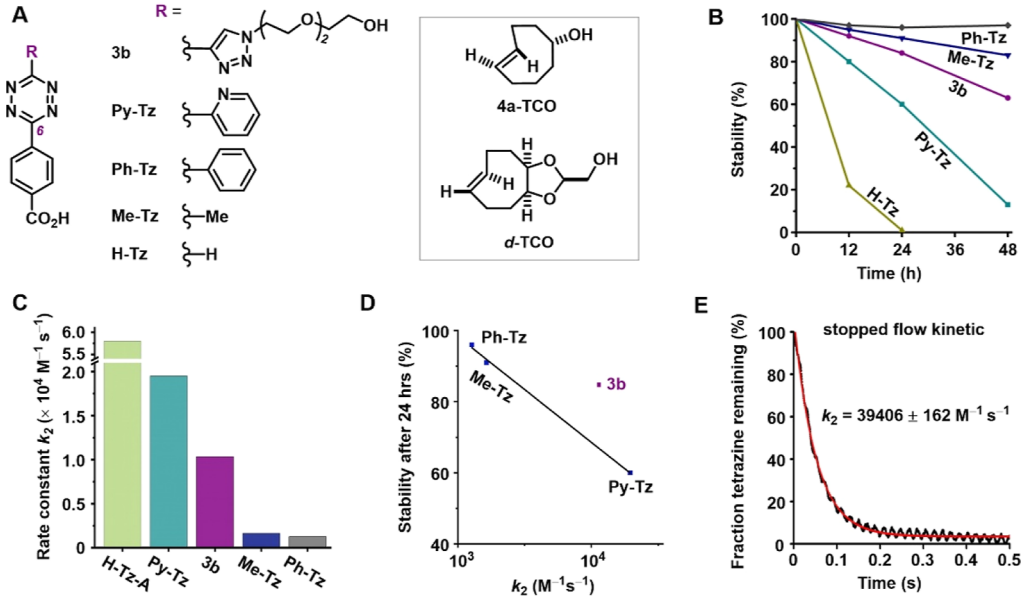

Figure 2. Comparison of stability and reactivity of triazolyl-tetrazine **3b** with other tetrazines. (A) Structures of the tetrazines and TCOs in this stability and reactivity study. (B) The stability of the tetrazines was evaluated in DMEM containing 10% FBS at 37 °C. (C) Second-order rate constants for the reactions of **H-Tz-A**,[44] **3b**, **Py-Tz**, **Me-Tz**, and **Ph-Tz** with 4a-TCO in PBS at 37 °C. (D) Correlation between the metabolic stability (residual fraction after 24 h incubation in DMEM) and reactivity of tetrazines. (E) Second-order rate constant for the reaction of **3b** with *d*-TCO in PBS at 23 °C.

distortion energy is the smallest (ΔE_{dist} = 17.8 kcal mol^{-1}). The ΔE_{dist} for **Ta-Tz** is 19.0 kcal mol^{-1}, which is lower by 1.7 kcal mol^{-1} than that for **Ph-Tz** (ΔE_{dist} = 20.7 kcal mol^{-1}). This finding agrees with the higher reactivity of **Ta-Tz** than **Ph-Tz** toward TCO. Recently, the Mikula group[29] explained the high reactivity of **Py-Tz** by the intramolecular repulsive N–N

https://doi.org/10.1021/jacsau.3c00843
JACS Au 2024, 4, 2853–2861

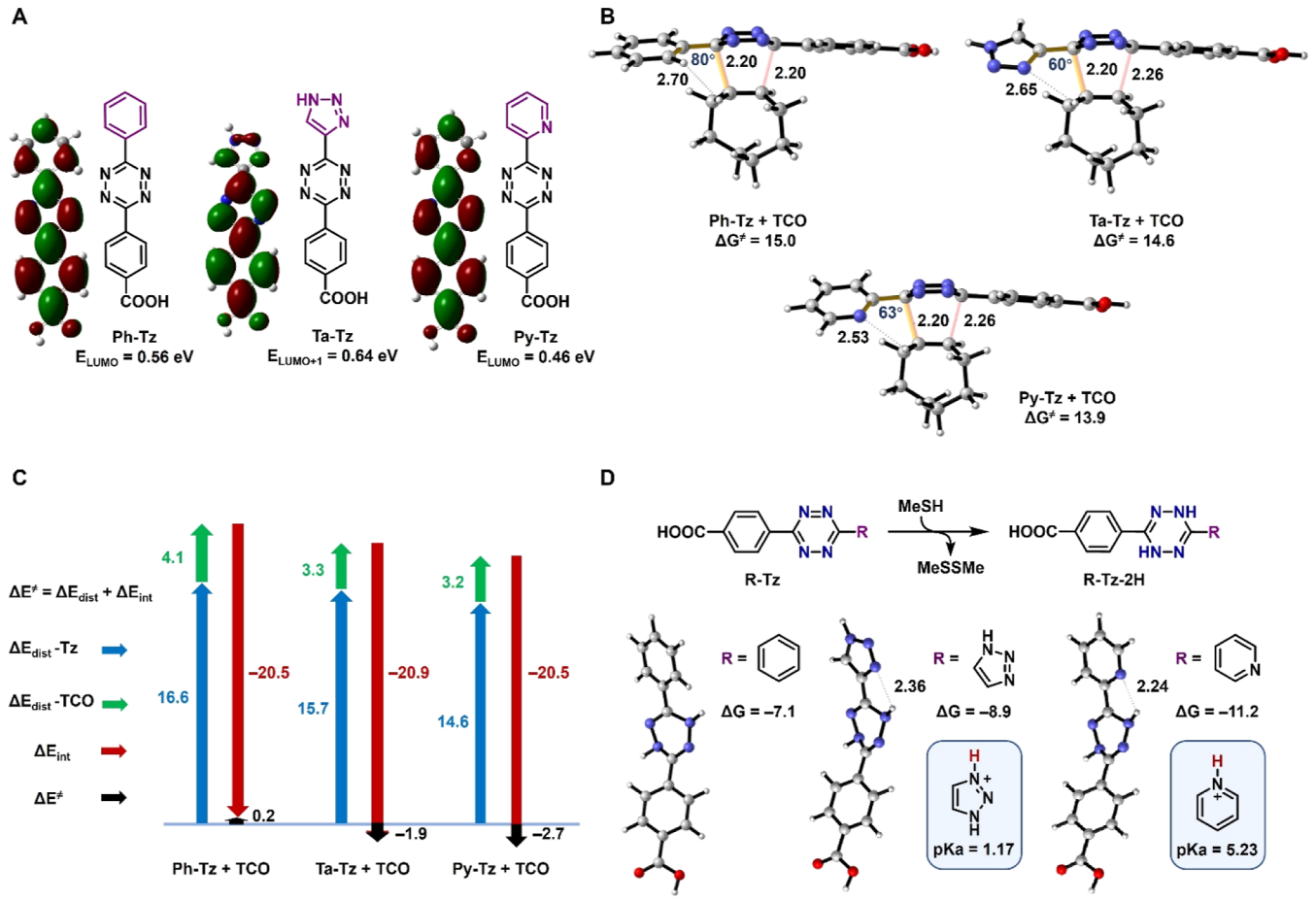

Figure 3. Theoretical calculations of three tetrazines. (A) LUMO or LUMO + 1 orbitals and orbital energies of substituted tetrazines were calculated at the HF/6-311+G(d,p)//M06-2*X*/6-31G(d) level of theory. (B) Computed transition-state geometries and activation free energies ($\Delta G^{\ddagger}$, kcal mol^{-1}) at the CPCM(water)-M06-2*X*/6-311+G(d,p)//M06-2*X*/6-31G(d) level of theory. (C) Distortion/interaction analysis of the reactions (ΔE, kcal mol^{-1}). (D) Energetics of the reduction of tetrazines by methanethiol (ΔG, kcal mol^{-1}).

interaction between its pyridyl and tetrazine moieties. The distinctive performance of **Ta-Tz** also benefits from the lower distortion energy introduced by the N−N repulsion. As shown in Figure 3B, in the structure of the transition state of the cycloaddition between **Ta-Tz** and TCO, the labeled dihedral angel is 60°, which is very close to that involving **Py-Tz** (63°).

The instability of tetrazines is usually attributed to two main potential reactions: attack by nucleophiles[49] and reduction to 2H-tetrazines.[50] As depicted in Figure 3A, the energy of the reacting vacant orbital of **Ta-Tz** is 0.64 eV, which is the highest among the three tetrazines. This means that **Ta-Tz** is less likely to be attacked by nucleophiles as compared to **Py-Tz**. In addition, we calculated the energetics of tetrazines to be reduced by methanethiol. The formation of **Py-Tz-2H** is the most exergonic (ΔG = −11.2 kcal mol^{-1}), indicating that **Py-Tz** is the most unstable tetrazine in the presence of biological reductants. According to the computational results, **Ta-Tz** (ΔG = −8.9 kcal mol^{-1}) is expected to be more stable than **Py-Tz**. While the stabilizing N···H hydrogen bond formation is observed in both **Ta-Tz-2H** and **Py-Tz-2H** (Figure 3D), the distance is longer (2.36 versus 2.24 Å), and the bond is much weaker in **Ta-Tz-2H** due to the less basicity of the triazolyl group (the pK_a values of protonated triazole and pyridine are 1.17 and 5.23, respectively[51]). Overall, our calculations explain why the newly designed triazolyl-tetrazines exhibit high reactivity and high stability. Compared to 2-pyridyl, a triazolyl group can also reduce the distortion energy by introducing N−N repulsion, ensuring the high cycloaddition reactivity of tetrazine. However, its weaker electron-withdrawing effect and basicity prevent the tetrazine from being attacked by nucleophiles and reduction to 2H-tetrazines.

To demonstrate the biomedical utility potential of this triazolyl-tetrazine compound, several proof-of-concept experiments were conducted (Figure 4). First, we assessed the feasibility of utilizing triazolyl-tetrazine derivatives for biomolecular modification and bioorthogonal labeling. Compound **3o**, which contains a BODIPY fluorophore and an active ester, can be readily attached to bovine serum albumin (BSA), resulting in the formation of an albumin−BODIPY conjugate (**BSA-3o**). Subsequently, this conjugate underwent bioorthogonal modification with a commercial fluorescent dye, **4e-TCO-Cy5**, leading to the dual-labeled conjugate **BSA-3o-Cy5** (Figures 4B and Supporting Information, S16).

Next, live cell labeling was performed on SKOV3 cells. Upon administering the fluorescent probe **3p** to SKOV3 cells pretargeted with *d*-TCO-triphenylphosphonium conjugates (***d*-TCO-TPP**),[52] we visualized a strong and specific fluorescence signal inside live cells within 1 min (Figures 4C and Supporting Information, S17A). The labeling colocalized with the commercial dye Mito-Tracker Red (Supporting Information, Figure S17B). These findings confirmed the cell permeability and bioorthogonal reactivity of triazolyl-tetra-

https://doi.org/10.1021/jacsau.3c00843
JACS Au 2024, 4, 2853−2861

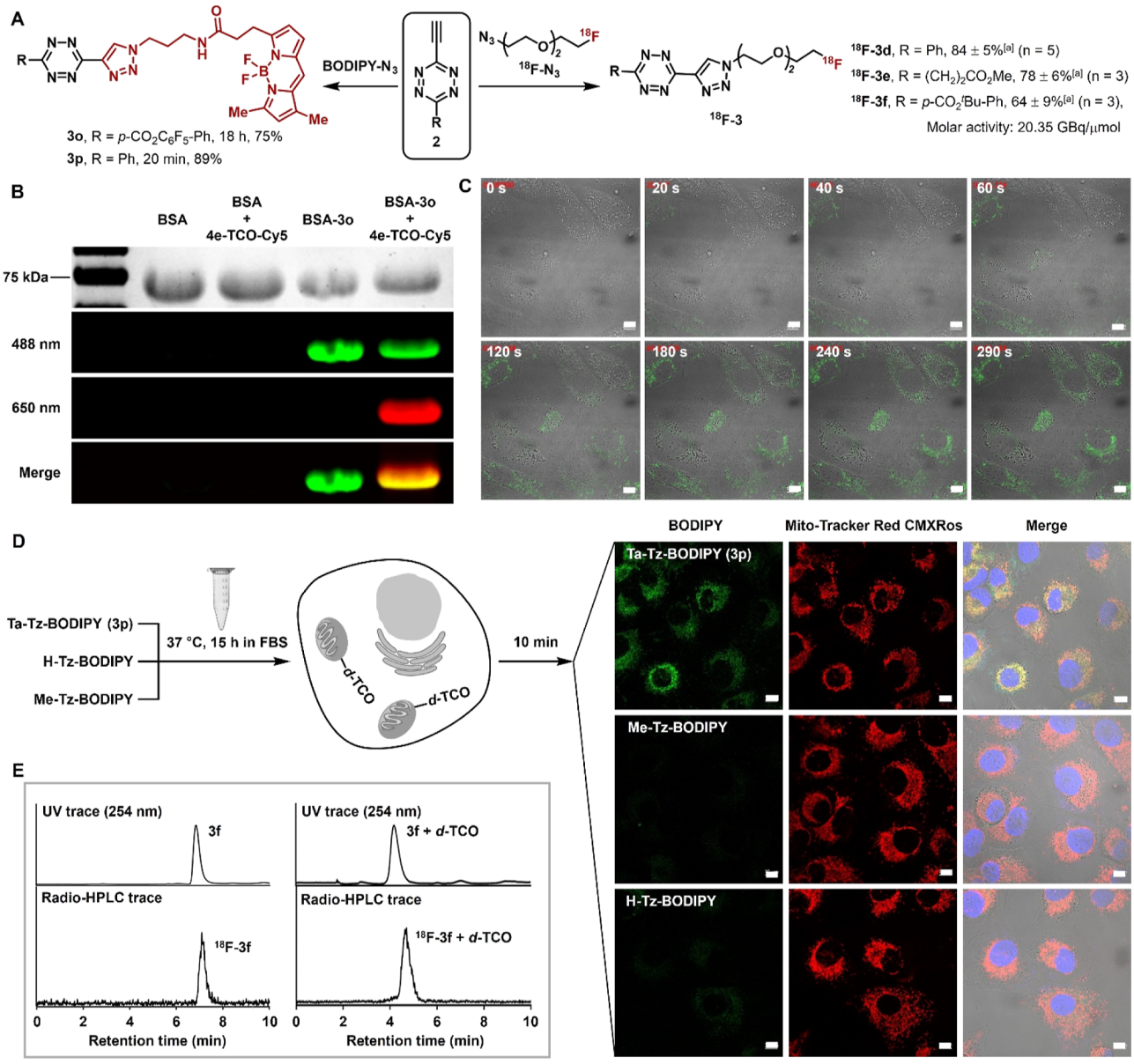

Figure 4. (A) Synthesis of functionalized triazolyl-tetrazines for diverse applications. [a]Decay-corrected radiochemical yields are indicated. (B) In-gel fluorescence analysis upon dual labeling of a protein. Gel analysis of BSA or **BSA-3o** alone or modified with **4e-TCO-Cy5** for 60 min in PBS. The upper panel shows Coomassie staining. (C) Time course imaging using probe **3p** (100 nM) in live SKOV3 cells, which are pretreated with *d*-**TCO-TPP**. Scale bar: 10 μm. (D) Imaging live SKOV3 cells using tetrazine probes **3p**, **Me-Tz-BODIPY**, and **H-Tz-BODIPY**. Tetrazines were preincubated in FBS at 37 °C for 15 h before treating cells. Cells were pretargeted by *d*-**TCO-TPP**, washed, labeled with tetrazines, and treated with Mito-Tracker Red as a colocalization reference. Scale bar: 10 μm. (E) The HPLC and radio-HPLC chromatograms show probe **3f** or ^{18}**F-3f** before (left) or after (right) reaction with *d*-TCO following a 2 h incubation in DMEM at 25 °C.

zines. Moreover, to investigate the balance between reactivity and stability of triazolyl-tetrazines, we selected two commercially available tetrazine-BODIPY probes, one bearing methyl and the other hydrogen substituents, respectively, as analogues of probe **3p** for comparison (see details in Figure S18). We incubated the three probes in FBS at 37 °C for 15 h to mimic the extended circulation and distribution duration of biomacromolecules in vivo. Subsequently, cells pretargeted with *d*-**TCO-TPP** were treated with the tetrazine probes and imaged using a confocal microscope. We observed significantly stronger mitochondrial staining within 10 min in cells treated with **3p**, with signals 10.3-fold and 2.5-fold higher than those from groups treated with **Me-Tz-BODIPY** and **H-Tz-BODIPY**, respectively (Figures 4D; Supporting Information, S18). These results demonstrate that triazolyl-tetrazines can maintain superb bioorthogonal reactivity under long-term physiological challenge conditions.

Finally, we investigated the application of this method to the synthesis of ^{18}F-labeled tetrazines, which exhibit promising potential for positron emission tomography (PET) imaging.[1,53] We envision that this click strategy could improve the radiolabeling yield by utilizing much easier-to-synthesize ^{18}F-azide precursors. With ^{18}F−N_3, ethynyl-tetrazine exhibited excellent radiochemical conversion (up to 95%). The desired ^{18}**F-3d** was isolated as a single product in 84 ± 5% yield (decay-corrected), which is improved compared with a previous report.[44] Its radiochemical purity exceeded 99% in each of five replicates (Figure 4A; Supporting Information,

https://doi.org/10.1021/jacsau.3c00843
JACS Au 2024, 4, 2853−2861

Table S4 and Figure S19). Furthermore, we evaluated the in vitro stability of ^{18}**F-3f**. This compound was found to remain stable in DMEM containing FBS, retaining its reactivity with *d*-TCO after a 2 h incubation in this physiological milieu (Figure 4E, Supporting Information, Figure S22).

This modular click strategy also allows for fine-tuning the hydrophilicity of the tetrazine probe, influencing its biodistribution performance and potentially increasing its clinical applicability (Figure 4A; Supporting Information, Tables S4−S6 and Figures S19−S21). Specifically, tracers ^{18}**F-3d** (predicted log *P* = 1.26) and ^{18}**F-3f** (predicted log *P* = 2.62) were administered to mice for micro-PET/CT imaging (Supporting Information, Figure S23). In comparison with ^{18}**F-3f**, the less hydrophobic tracer ^{18}**F-3d** exhibits a more rapid clearance rate from the liver. Radioactivity in the liver gradually transferred to the lower digestive tract and urinary system for 55 min postinjection, with approximately 60% of injected radioactivity accumulating in the urinary system at the end of the scan. The hepatic/renal ratio of ^{18}**F-3d** decreased from 1.86 at 5 min to 0.26 at 55 min, whereas the corresponding ratio for ^{18}**F-3f** remained nearly constant around 0.80.

CONCLUSIONS

In summary, we have developed an approach for generating triazolyl-tetrazines in a modular and scalable manner from a series of shelf-stable ethynyl-tetrazines. This copper-catalyzed click strategy enables the straightforward creation of versatile functional tetrazine probes in most laboratory settings. The resulting triazolyl-tetrazines exhibit both good stability and high reactivity under physiological conditions, overcoming the challenges of accessibility and compatibility between stability and reactivity faced by existing tetrazine probes. As a proof of their biomedical usefulness, our pilot studies demonstrate the biocompatibility and permeability for live cell labeling. Additionally, this versatile approach can be used to construct radiolabeled bioorthogonal probes with high radiochemical yields, also enabling the fine-tuning of pharmacokinetic properties through structural variation of substituents and functional groups. Our approach is easy to implement and leverages the commercial availability of azides with substantial substrate scope, promising access to diverse tetrazine probes for biomedical research, materials science, and theranostics.

METHODS

General Procedure for Ethynyl-Tetrazines

To a mixture of $PdCl_2(PPh_3)_2$ (28.0 mg, 0.04 mmol, 20 mol %) and CuI (76.2 mg, 0.4 mmol, 2.0 equiv) in 1,4-dioxane (2.0 mL) were successively added tetrazine **1** (0.2 mmol, 1.0 equiv) and tributyl-(trimethylsilylethynyl)stannane (147 μL, 0.4 mmol, 2.0 equiv) under an argon atmosphere. The reaction mixture was heated at 50 °C for 12 h. After reaction completion, as monitored by thin-layer chromatography (TLC), the reaction mixture was concentrated under reduced pressure and the residue was subjected to silica gel column chromatography (PE/EtOAc = 50:1 to 5:1) to afford the corresponding crude product. The crude product was dissolved in MeOH (10 mL), and K_2CO_3 (2.8 mg, 0.1 equiv) was added. The mixture was stirred at room temperature for 1−5 min. After reaction completion as monitored by TLC, the reaction was immediately extracted with DCM (3 × 20 mL) and washed with brine. (Caution! Dry solvent is necessary and when the reaction is completed, it needs to be worked up immediately). The combined organic extracts were dried with anhydrous Na_2SO_4, filtered, and concentrated under reduced pressure and the residue was purified by silica gel column chromatography (PE/EtOAc = 50:1 to 5:1) to afford the corresponding product ethynyl-tetrazines **2**.

General Procedure for Triazolyl-Tetrazines

A mixture of $CuSO_4$ (0.1 equiv), tris(3-hydroxypropyltriazolylmethyl)amine (0.1 equiv), and sodium ascorbate (0.2 equiv) in 2 mL of DMF/H_2O (4:1) was stirred at room temperature for 10 min. Then, azide (10 mg, 1.0 equiv) and ethynyl-tetrazine **2** (1.0 equiv) were added. The reaction mixture was stirred at room temperature. After reaction completion, as monitored by TLC, the reaction was worked up to afford the corresponding product.

ASSOCIATED CONTENT

Supporting Information

The Supporting Information is available free of charge at https://pubs.acs.org/doi/10.1021/jacsau.3c00843.

General experimental considerations, synthetic procedures, computational methods, reaction kinetics, compound stability and characterization, and copies of NMR spectra (PDF)

AUTHOR INFORMATION

Corresponding Authors

Yong Liang − *State Key Laboratory of Coordination Chemistry, Jiangsu Key Laboratory of Advanced Organic Materials, School of Chemistry and Chemical Engineering, Chemistry and Biomedicine Innovation Center, Nanjing University, Nanjing 210023, China;* orcid.org/0000-0001-5026-6710; Email: yongliang@nju.edu.cn

Haoxing Wu − *Department of Radiology and Huaxi MR Research Center, Functional and Molecular Imaging Key Laboratory of Sichuan Province and Frontiers Science Center for Disease Related Molecular Network, West China Hospital, Sichuan University, Chengdu 610041, China; Key Laboratory of Drug-Targeting and Drug Delivery System of the Education Ministry and Sichuan Province, Sichuan University, Chengdu 610041, China;* orcid.org/0000-0002-0008-4668; Email: haoxingwu@scu.edu.cn

Authors

Haojie Yang − *Department of Radiology and Huaxi MR Research Center, Functional and Molecular Imaging Key Laboratory of Sichuan Province and Frontiers Science Center for Disease Related Molecular Network, West China Hospital, Sichuan University, Chengdu 610041, China*

Hongbao Sun − *Department of Radiology and Huaxi MR Research Center, Functional and Molecular Imaging Key Laboratory of Sichuan Province and Frontiers Science Center for Disease Related Molecular Network, West China Hospital, Sichuan University, Chengdu 610041, China;* orcid.org/0000-0002-7956-0232

Yinghan Chen − *State Key Laboratory of Coordination Chemistry, Jiangsu Key Laboratory of Advanced Organic Materials, School of Chemistry and Chemical Engineering, Chemistry and Biomedicine Innovation Center, Nanjing University, Nanjing 210023, China;* orcid.org/0000-0002-7897-7626

Yayue Wang − *Department of Radiology and Huaxi MR Research Center, Functional and Molecular Imaging Key Laboratory of Sichuan Province and Frontiers Science Center for Disease Related Molecular Network, West China Hospital, Sichuan University, Chengdu 610041, China*

https://doi.org/10.1021/jacsau.3c00843
JACS Au 2024, 4, 2853−2861

Cheng Yang − *Key Laboratory of Drug-Targeting and Drug Delivery System of the Education Ministry and Sichuan Province, Sichuan University, Chengdu 610041, China*
Fang Yuan − *Department of Radiology and Huaxi MR Research Center, Functional and Molecular Imaging Key Laboratory of Sichuan Province and Frontiers Science Center for Disease Related Molecular Network, West China Hospital, Sichuan University, Chengdu 610041, China*
Xiaoai Wu − *Department of Nuclear Medicine and Clinical Nuclear Medicine Research Lab, West China Hospital, Sichuan University, Chengdu 610041, China;* orcid.org/0000-0002-3518-9689
Wei Chen − *Department of Nuclear Medicine and Clinical Nuclear Medicine Research Lab, West China Hospital, Sichuan University, Chengdu 610041, China*
Ping Yin − *School of Materials Science & Engineering, Beijing Institute of Technology, Beijing 100081, China;* orcid.org/0000-0002-2870-8225

Complete contact information is available at: https://pubs.acs.org/10.1021/jacsau.3c00843

Author Contributions

Haojie Yang, Hongbao Sun, and Yinghan Chen contributed equally. The manuscript was written through contributions of all authors. All authors have given approval to the final version of the manuscript.

Notes

The authors declare no competing financial interest.

■ ACKNOWLEDGMENTS

This work was supported by the National Natural Science Foundation of China (22377083, 22271200, 22077062, and 21801178), the Natural Science Foundation of Sichuan, China (2023NSFSC1716 and 2023NSFSC0645), and the 1.3.5 Project for Disciplines of Excellence at West China Hospital, Sichuan University (ZYYC23003). We thank Feijing Su and Qifeng Liu at the Core Facilities of West China Hospital and Xiaoyan Wang and Yuanming Zhai at the Analytical & Testing Center of Sichuan University for their help with NMR measurements. We thank the High Performance Computing Center (HPCC) of Nanjing University for doing the numerical calculations in this paper on its blade cluster system.

■ REFERENCES

(1) Scinto, S. L.; Bilodeau, D. A.; Hincapie, R.; Lee, W.; Nguyen, S. S.; Xu, M.; Am Ende, C. W.; Finn, M. G.; Lang, K.; Lin, Q.; Pezacki, J. P.; Prescher, J. A.; Robillard, M. S.; Fox, J. M. Bioorthogonal chemistry. *Nat. Rev. Methods Primers* **2021**, *1*, 30.
(2) Devaraj, N. K. The Future of Bioorthogonal Chemistry. *ACS Cent. Sci.* **2018**, *4*, 952−959.
(3) Bertozzi, C. R. A decade of bioorthogonal chemistry. *Acc. Chem. Res.* **2011**, *44*, 651−653.
(4) Sletten, E. M.; Bertozzi, C. R. Bioorthogonal chemistry: fishing for selectivity in a sea of functionality. *Angew. Chem., Int. Ed.* **2009**, *48*, 6974−6998.
(5) Saxon, E.; Bertozzi, C. R. Cell Surface Engineering by a Modified Staudinger Reaction. *Science* **2000**, *287*, 2007−2010.
(6) Nguyen, S. S.; Prescher, J. A. Developing bioorthogonal probes to span a spectrum of reactivities. *Nat. Rev. Chem* **2020**, *4*, 476−489.
(7) Selvaraj, R.; Fox, J. M. Trans-Cyclooctene—a stable, voracious dienophile for bioorthogonal labeling. *Curr. Opin. Chem. Biol.* **2013**, *17*, 753−760.
(8) Rigolot, V.; Biot, C.; Lion, C. To View Your Biomolecule, Click inside the Cell. *Angew. Chem., Int. Ed.* **2021**, *60*, 23084−23105.
(9) Wang, J.; Wang, X.; Fan, X.; Chen, P. R. Unleashing the Power of Bond Cleavage Chemistry in Living Systems. *ACS Cent. Sci.* **2021**, *7*, 929−943.
(10) Ji, X.; Pan, Z.; Yu, B.; De La Cruz, L. K.; Zheng, Y.; Ke, B.; Wang, B. Click and release: bioorthogonal approaches to "on-demand" activation of prodrugs. *Chem. Soc. Rev.* **2019**, *48*, 1077−1094.
(11) Versteegen, R. M.; Rossin, R.; ten Hoeve, W.; Janssen, H. M.; Robillard, M. S. Click to Release: Instantaneous Doxorubicin Elimination upon Tetrazine Ligation. *Angew. Chem., Int. Ed.* **2013**, *52*, 14112−14116.
(12) Li, J.; Chen, P. R. Development and application of bond cleavage reactions in bioorthogonal chemistry. *Nat. Chem. Biol.* **2016**, *12*, 129−137.
(13) Wang, Y.; Shen, G.; Li, J.; Mao, W.; Sun, H.; Feng, P.; Wu, H. Bioorthogonal Cleavage of Tetrazine-Caged Ethers and Esters Triggered by trans-Cyclooctene. *Org. Lett.* **2022**, *24*, 5293−5297.
(14) Peplow, M. 'Clicked' drugs: researchers prove the remarkable chemistry in humans. *Nat. Biotechnol.* **2023**, *41*, 883−885.
(15) Shieh, P.; Bertozzi, C. R. Design strategies for bioorthogonal smart probes. *Org. Bio. Chem.* **2014**, *12*, 9307−9320.
(16) Oliveira, B. L.; Guo, Z.; Bernardes, G. J. L. Inverse electron demand Diels-Alder reactions in chemical biology. *Chem. Soc. Rev.* **2017**, *46*, 4895−4950.
(17) van Onzen, A. H. A. M.; Versteegen, R. M.; Hoeben, F. J. M.; Filot, I. A. W.; Rossin, R.; Zhu, T.; Wu, J.; Hudson, P. J.; Janssen, H. M.; ten Hoeve, W.; Robillard, M. S. Bioorthogonal Tetrazine Carbamate Cleavage by Highly Reactive trans-Cyclooctene. *J. Am. Chem. Soc.* **2020**, *142*, 10955−10963.
(18) Blackman, M. L.; Royzen, M.; Fox, J. M. Tetrazine Ligation: Fast Bioconjugation Based on Inverse-Electron-Demand Diels-Alder Reactivity. *J. Am. Chem. Soc.* **2008**, *130*, 13518−13519.
(19) Darko, A.; Wallace, S.; Dmitrenko, O.; Machovina, M. M.; Mehl, R. A.; Chin, J. W.; Fox, J. M. Conformationally Strained trans-Cyclooctene with Improved Stability and Excellent Reactivity in Tetrazine Ligation. *Chem. Sci.* **2014**, *5*, 3770−3776.
(20) Srinivasan, S.; Yee, N. A.; Wu, K.; Zakharian, M.; Mahmoodi, A.; Royzen, M.; Oneto, J. M. M. SQ3370 Activates Cytotoxic Drug via Click Chemistry at Tumor and Elicits Sustained Responses in Injected and Non-Injected Lesions. *Adv. Ther.* **2021**, *4*, 2000243.
(21) Wu, K.; Yee, N. A.; Srinivasan, S.; Mahmoodi, A.; Zakharian, M.; Mejia Oneto, J. M.; Royzen, M. Click activated protodrugs against cancer increase the therapeutic potential of chemotherapy through local capture and activation. *Chem. Sci.* **2021**, *12*, 1259−1271.
(22) Werther, P.; Yserentant, K.; Braun, F.; Grußmayer, K.; Navikas, V.; Yu, M.; Zhang, Z.; Ziegler, M. J.; Mayer, C.; Gralak, A. J.; Busch, M.; Chi, W.; Rominger, F.; Radenovic, A.; Liu, X.; Lemke, E. A.; Buckup, T.; Herten, D.-P.; Wombacher, R. Bio-orthogonal Red and Far-Red Fluorogenic Probes for Wash-Free Live-Cell and Super-resolution Microscopy. *ACS Cent. Sci.* **2021**, *7*, 1561−1571.
(23) McFarland, J. M.; Alečković, M.; Coricor, G.; Srinivasan, S.; Tso, M.; Lee, J.; Nguyen, T.-H.; Mejía Oneto, J. M. Click Chemistry Selectively Activates an Auristatin Protodrug with either Intratumoral or Systemic Tumor-Targeting Agents. *ACS Cent. Sci.* **2023**, *9*, 1400−1408.
(24) Yao, Q.; Lin, F.; Fan, X.; Wang, Y.; Liu, Y.; Liu, Z.; Jiang, X.; Chen, P. R.; Gao, Y. Synergistic enzymatic and bioorthogonal reactions for selective prodrug activation in living systems. *Nat. Commun.* **2018**, *9*, 5032.
(25) Wang, Y.; Zhang, J.; Han, B.; Tan, L.; Cai, W.; Li, Y.; Su, Y.; Yu, Y.; Wang, X.; Duan, X.; Wang, H.; Shi, X.; Wang, J.; Yang, X.; Liu, T. Noncanonical amino acids as doubly bio-orthogonal handles for one-pot preparation of protein multiconjugates. *Nat. Commun.* **2023**, *14*, 974.
(26) García-Vázquez, R.; Battisti, U. M.; Jørgensen, J. T.; Shalgunov, V.; Hvass, L.; Stares, D. L.; Petersen, I. N.; Crestey, F.; Löffler, A.; Svatunek, D.; Kristensen, J. L.; Mikula, H.; Kjaer, A.; Herth, M. M.

Direct Cu-mediated aromatic ^{18}F-labeling of highly reactive tetrazines for pretargeted bioorthogonal PET imaging. *Chem. Sci.* **2021**, *12*, 11668−11675.
(27) Clavier, G.; Audebert, P. *s*-Tetrazines as Building Blocks for New Functional Molecules and Molecular Materials. *Chem. Rev.* **2010**, *110*, 3299−3314.
(28) Xie, Y.; Fang, Y.; Huang, Z.; Tallon, A. M.; am Ende, C. W.; Fox, J. M. Divergent Synthesis of Monosubstituted and Unsymmetrical 3,6-Disubstituted Tetrazines from Carboxylic Ester Precursors. *Angew. Chem., Int. Ed.* **2020**, *59*, 16967−16973.
(29) Svatunek, D.; Wilkovitsch, M.; Hartmann, L.; Houk, K. N.; Mikula, H. Uncovering the Key Role of Distortion in Bioorthogonal Tetrazine Tools that Defy the Reactivity/Stability Trade-Off. *J. Am. Chem. Soc.* **2022**, *144*, 8171−8177.
(30) Yang, J.; Karver, M. R.; Li, W.; Sahu, S.; Devaraj, N. K. Metal-Catalyzed One-Pot Synthesis of Tetrazines Directly from Aliphatic Nitriles and Hydrazine. *Angew. Chem., Int. Ed.* **2012**, *51*, 5222−5225.
(31) Mao, W.; Shi, W.; Li, J.; Su, D.; Wang, X.; Zhang, L.; Pan, L.; Wu, X.; Wu, H. Organocatalytic and Scalable Syntheses of Unsymmetrical 1,2,4,5-Tetrazines by Thiol-Containing Promotors. *Angew. Chem., Int. Ed.* **2019**, *58*, 1106−1109.
(32) Qu, Y.; Sauvage, F. X.; Clavier, G.; Miomandre, F.; Audebert, P. Metal-Free Synthetic Approach to 3-Monosubstituted Unsymmetrical 1,2,4,5-Tetrazines Useful for Bioorthogonal Reactions. *Angew. Chem., Int. Ed.* **2018**, *57*, 12057−12061.
(33) Wieczorek, A.; Werther, P.; Euchner, J.; Wombacher, R. Green-to far-red-emitting Fluorogenic Tetrazine Probes-Synthetic Access and No-wash Protein Imaging inside Living Cells. *Chem. Sci.* **2017**, *8*, 1506−1510.
(34) Wu, H.; Yang, J.; Seckute, J.; Devaraj, N. K. In Situ Synthesis of Alkenyl Tetrazines for Highly Fluorogenic Bioorthogonal Live-Cell Imaging Probes. *Angew. Chem., Int. Ed.* **2014**, *53*, 5805−5809.
(35) Lambert, W. D.; Fang, Y.; Mahapatra, S.; Huang, Z.; am Ende, C. W.; Fox, J. M. Installation of Minimal Tetrazines through Silver-Mediated Liebeskind-Srogl Coupling with Arylboronic Acids. *J. Am. Chem. Soc.* **2019**, *141*, 17068−17074.
(36) Testa, C.; Gigot, E.; Genc, S.; Decreau, R.; Roger, J.; Hierso, J. C. *Ortho*-Functionalized Aryltetrazines by Direct Palladium-Catalyzed C-H Halogenation: Application to Fast Electrophilic Fluorination Reactions. *Angew. Chem., Int. Ed.* **2016**, *55*, 5555−5559.
(37) Creary, X.; Chormanski, K.; Peirats, G.; Renneburg, C. Electronic Properties of Triazoles. Experimental and Computational Determination of Carbocation and Radical-Stabilizing Properties. *J. Org. Chem.* **2017**, *82*, 5720−5730.
(38) Novák, Z.; Kotschy, A. First Cross-Coupling Reactions on Tetrazines. *Org. Lett.* **2003**, *5*, 3495−3497.
(39) Ros, E.; Prades, A.; Forson, D.; Smyth, J.; Verdaguer, X.; Pouplana, L. R. d.; Riera, A. Synthesis of 3-alkyl-6-methyl-1,2,4,5-tetrazines *via* a Sonogashira-type cross-coupling reaction. *Chem. Commun.* **2020**, *56*, 11086−11089.
(40) Presolski, S. I.; Hong, V.; Cho, S.-H.; Finn, M. G. Tailored Ligand Acceleration of the Cu-Catalyzed Azide-Alkyne Cycloaddition Reaction: Practical and Mechanistic Implications. *J. Am. Chem. Soc.* **2010**, *132*, 14570−14576.
(41) Besanceney-Webler, C.; Jiang, H.; Zheng, T.; Feng, L.; del Amo, D. S.; Wang, W.; Klivansky, L. M.; Marlow, F. L.; Liu, Y.; Wu, P. Increasing the Efficacy of Bioorthogonal Click Reactions for Bioconjugation: A Comparative Study. *Angew. Chem., Int. Ed.* **2011**, *50*, 8051−8056.
(42) Majano, G.; Mintova, S.; Bein, T.; Klapötke, T. High-Density Energetic Material Hosted in Pure Silica MFI-Type Zeolite Nanocrystals. *Adv. Mater.* **2006**, *18*, 2440−2443.
(43) Chavez, D. E.; Parrish, D. A.; Mitchell, L.; Imler, G. H. Azido and Tetrazolo 1,2,4,5-Tetrazine N-Oxides. *Angew. Chem., Int. Ed.* **2017**, *56*, 3575−3578.
(44) Steen, E. J. L.; Jørgensen, J. T.; Denk, C.; Battisti, U. M.; Nørregaard, K.; Edem, P. E.; Bratteby, K.; Shalgunov, V.; Wilkovitsch, M.; Svatunek, D.; Poulie, C. B. M.; Hvass, L.; Simon, M.; Wanek, T.; Rossin, R.; Robillard, M.; Kristensen, J. L.; Mikula, H.; Kjaer, A.; Herth, M. M. Lipophilicity and Click Reactivity Determine the Performance of Bioorthogonal Tetrazine Tools in Pretargeted In Vivo Chemistry. *ACS Pharmacol. Transl. Sci.* **2021**, *4*, 824−833.
(45) Liu, F.; Liang, Y.; Houk, K. N. Theoretical Elucidation of the Origins of Substituent and Strain Effects on the Rates of Diels-Alder Reactions of 1,2,4,5-Tetrazines. *J. Am. Chem. Soc.* **2014**, *136*, 11483−11493.
(46) Bickelhaupt, F. M.; Houk, K. N. Analyzing Reaction Rates with the Distortion/Interaction-Activation Strain Model. *Angew. Chem., Int. Ed.* **2017**, *56*, 10070−10086.
(47) Liu, F.; Liang, Y.; Houk, K. N. Bioorthogonal Cycloadditions: Computational Analysis with the Distortion/Interaction Model and Predictions of Reactivities. *Acc. Chem. Res.* **2017**, *50*, 2297−2308.
(48) Ess, D. H.; Houk, K. N. Theory of 1,3-Dipolar Cycloadditions: Distortion/Interaction and Frontier Molecular Orbital Models. *J. Am. Chem. Soc.* **2008**, *130*, 10187−10198.
(49) Kämpchen, T.; Massa, W.; Overheu, W.; Schmidt, R.; Seitz, G. Zur Kenntnis von Reaktionen des 1,2,4,5-Tetrazin-3,6-dicarbonsäure-dimethylesters mit Nucleophilen. *Chem. Ber.* **1982**, *115*, 683−694.
(50) Zhao, Z.; Cao, L.; Zhang, T.; Hu, R.; Wang, S.; Li, S.; Li, Y.; Yang, G. Novel Reaction-Based Fluorescence Probes for the Detection of Hydrogen Sulfide in Living Cells. *ChemistrySelect* **2016**, *1*, 2581−2585.
(51) Tshepelevitsh, S.; Kütt, A.; Lõkov, M.; Kaljurand, I.; Saame, J.; Heering, A.; Plieger, P. G.; Vianello, R.; Leito, I. On the Basicity of Organic Bases in Different Media. *Eur. J. Org Chem.* **2019**, *40*, 6735−6748.
(52) Mao, W.; Chi, W.; He, X.; Wang, C.; Wang, X.; Yang, H.; Liu, X.; Wu, H. Overcoming Spectral Dependence: A General Strategy for Developing Far-Red and Near-Infrared Ultra-Fluorogenic Tetrazine Bioorthogonal Probes. *Angew. Chem., Int. Ed.* **2022**, *61*, No. e202117386.
(53) Zhong, X.; Yan, J.; Ding, X.; Su, C.; Xu, Y.; Yang, M. Recent Advances in Bioorthogonal Click Chemistry for Enhanced PET and SPECT Radiochemistry. *Bioconjugate Chem.* **2023**, *34*, 457−476.

https://doi.org/10.1021/jacsau.3c00843
JACS Au 2024, 4, 2853−2861